THE JOURNAL OF BIOLOGICAL CHEMISTRY VOL. 286, NO. 29, pp. 25519–25530, July 22, 2011

Glycosylation Regulates Specific Induction of Rice Immune Responses by *Acidovorax avenae* Flagellin*[S]

Received for publication, April 22, 2011, and in revised form, May 19, 2011 Published, JBC Papers in Press, May 31, 2011, DOI 10.1074/jbc.M111.254029

Hiroyuki Hirai[‡], Ryota Takai[‡], Megumi Iwano[§], Masaru Nakai[§], Machiko Kondo[‡], Seiji Takayama[§], Akira Isogai[§], and Fang-Sik Che[‡§1]

From the [‡]Graduate School of Bio-Science, Nagahama Institute of Bio-Science and Technology, 1266 Tamura, Nagahama, Shiga 526-0829, Japan and the [§]Graduate School of Biological Sciences, Nara Institute of Science and Technology (NAIST), 8916-5 Takayama, Ikoma, Nara 630-0101, Japan

Plants have a sensitive system that detects various pathogen-derived molecules to protect against infection. Flagellin, a main component of the bacterial flagellum, from the rice avirulent N1141 strain of the Gram-negative phytopathogenic bacterium *Acidovorax avenae* induces plant immune responses including H_2O_2 generation, whereas flagellin from the rice virulent K1 strain of *A. avenae* does not induce these immune responses. To clarify the molecular mechanism that leads to these differing responses between the K1 and N1141 flagellins, recombinant K1 and N1141 flagellins were generated using an *Escherichia coli* expression system. When cultured rice cells were treated with recombinant K1 or N1141 flagellin, both flagellins equally induced H_2O_2 generation, suggesting that post-translational modifications of the flagellins are involved in the specific induction of immune responses. Mass spectrometry analyses using glycosyltransferase-deficient mutants showed that 1,600- and 2,150-Da glycans were present on the flagellins from N1141 and K1, respectively. A deglycosylated K1 flagellin induced immune responses in the same manner as N1141 flagellin. Site-directed mutagenesis revealed that glycans were attached to four amino acid residues (Ser^{178}, Ser^{183}, Ser^{212}, and Thr^{351}) in K1 flagellin. Among mutant K1 flagellins in which each glycan-attached amino acid residue was changed to alanine, S178A and S183A, K1 flagellin induced a strong immune response in cultured rice cells, indicating that the glycans at Ser^{178} and Ser^{183} in K1 flagellin prevent epitope recognition in rice.

During development, plants are continuously confronted with diverse pathogens. However, plants are resistant to most microbes and rely entirely on plant immune responses for their defense. Plants have evolved a multilayered defense system that can be activated upon pathogen invasion. The first layer recognizes conserved microbial molecules, referred to as microbe-associated molecular patterns, via pattern recognition receptors (1, 2). Microbe-associated molecular pattern-triggered immunity is key to plant innate immunity (3). Successful pathogens can deliver effectors that suppress these immune responses and contribute to pathogen virulence (4). Another layer recognizes pathogen effector molecules through host resistance genes, triggering a rapid defense response that often includes a localized programmed cell death reaction known as the hypersensitive response (5–7).

Microbe-associated molecular patterns include structures characteristic of pathogens, such as β-glucan, polysaccharide chitin, ergosterol, lipopolysaccharides (LPS), flagellin, and elongation factor Tu (8–13). Among these microbe-associated molecular patterns, flagellin, a main component of the bacterial flagellum, has been the most extensively studied in regard to the recognition mechanism and signal transduction. *Arabidopsis* recognizes the most conserved N-terminal domain of flagellin that consists of a 22-amino acid peptide (flg22)[2] (12). Recognition of this elicitor-active domain depends on flagellin sensing 2 (FLS2) (14). FLS2 encodes a receptor-like kinase composed of an extracellular leucine-rich repeat, a single membrane-spanning domain, and a cytoplasmic serine/threonine kinase domain. FLS2 and flg22 were shown to physically interact by chemical cross-linking and immunoprecipitation studies, suggesting that FLS2 determines the specificity in recognizing flagellin (15).

Acidovorax avenae is a Gram-negative bacterium that causes a seedling disease that is characterized by the formation of brown stripes on the sheaths of infected plants. *A. avenae* has a wide host range among monocotyledonous plants; however, individual strains of this pathogen infect only one or a few host species (16). For example, strains isolated from rice, such as K1 and H8301, can infect only rice plants (virulent), whereas the N1141 strain isolated from finger millet cannot infect rice even after it is inoculated into rice tissues (avirulent). We reported that a rice avirulent N1141 strain of *A. avenae* induces several immune responses, such as hypersensitive response cell death, H_2O_2 generation, and up-regulation of defense genes, whereas the rice virulent K1 and H8301 strains of *A. avenae* do not induce these immune responses (17–20). To identify the specific recognition molecules that are related to the induction of these immune responses in cultured rice cells, a strain-specific antibody was raised against the avirulent strain and then

* This work was supported in part by Grant-in-aid for Scientific Research (B) 21380073 from the Ministry of Education, Culture, Sports, Science and Technology of Japan and Grant 500107 from the Program for Promotion of Basic and Applied Researches for Innovations in Bio-oriented Industry.

[S] The on-line version of this article (available at http://www.jbc.org) contains supplemental Figs. 1–3.

[1] To whom correspondence should be addressed: Graduate School of Bio-Science, Nagahama Inst. of Bio-Science and Technology, 1266 Tamura, Nagahama, Shiga 526-0829, Japan. Tel.: 81-749-64-8162; Fax: 81-749-64-8140; E-mail: k_sai@nagahama-i-bio.ac.jp.

[2] The abbreviations used are: flg22, conserved N-terminal domain of flagellin that consists of a 22-amino acid peptide; FLS2, flagellin sensing 2; PAL, phenylalanine ammonia-lyase.

absorbed with the virulent strain. The specific antibody detected the flagellin protein, which is structurally different between the virulent and avirulent strains of *A. avenae* (21). Flagellin purified from the avirulent N1141 strain induced rice immune responses, whereas flagellin purified from the virulent K1 strain did not induce these responses. Furthermore, a flagellin-deficient N1141 strain lost the ability to induce immune responses. These data indicate that flagellin from the avirulent N1141 strain of *A. avenae* specifically induces immune responses in cultured rice cells.

Interestingly, neither flg22 nor flg22-avenae (comprising the flg22 position of N1141 flagellin) induced weak immune responses compared with flagellin from the rice avirulent N1141 strain (22). Full-length sequence analysis of the flagellins from the N1141 and K1 strains showed that both flagellins consisted of 492 amino acids, 14 of which differ between the N1141 and K1 flagellins. All of the substituted amino acid residues are between residues 178 and 382 and are not located in the N-terminal region containing flg22, suggesting that the epitope contributing to specific recognition in rice is present within a region other than flg22. Furthermore, mass spectrometry analysis and sugar chain analysis revealed that the flagellin proteins of the N1141 and H8301 strains were post-translationally glycosylated. The glycosylation pattern should be different between the N1141 and H8301 flagellins because the calculated and measured masses were different between the N1141 and H8301 flagellins (21). However, it is still unknown whether amino acid substitutions and sugar chain modifications in flagellin are involved in specific recognition by rice that induces immune responses.

Because the rice immune response, such as H_2O_2 generation, was only induced by the avirulent N1141 flagellin, we postulated that the specific induction of immune responses by *A. avenae* flagellins is due to a structural difference between the N1141 and K1 flagellins. Based on this hypothesis, recombinant N1141 and K1 flagellins were produced in *Escherichia coli*. Both N1141 recombinant flagellin and K1 recombinant flagellin induced specific immune responses, such as H_2O_2 generation, indicating that the induction specificity of the immune responses to flagellin is regulated by transcriptional sugar chain modifications. Here, we report that four amino acids residues are glycosylated in the flagellin from the rice virulent K1 strain and that glycosylation of flagellin may prevent epitope recognition in rice.

EXPERIMENTAL PROCEDURES

Plants and Bacteria—Suspension cultures of rice cells (line Oc) were grown at 30 °C under light irradiation (23). The cells were diluted in fresh medium every week, and all experiments were performed 3 or 4 days after transfer. *A. avenae* strains N1141 (MAFF 301141) and K1 (MAFF 301755) were used as described previously (16, 21).

Purification of Flagellin—Flagellin was purified as described previously with several modifications (21). The *A. avenae* strains N1141 and K1 were grown for 1.5 days in LB medium at 30 °C on a rotary shaker. The cells were harvested by centrifugation at 6,000 × *g* for 20 min at 4 °C. The cell pellets were washed with 20 mM Tris-HCl (pH 7.5) containing 137 mM NaCl and 2.68 mM KCl, collected by centrifugation, and then resuspended in 90 ml of the same buffer. Flagella were removed from the cells by shearing for 3 min in a homogenizer (Ultra F Homogenizer HF-93F, Taitec, Saitama, Japan). Intact cells and cellular debris were removed using a two-step centrifugation procedure at 6,000 × *g* for 30 min and 16,000 × *g* for 60 min at 4 °C. The flagella were collected by ultracentrifuging at 200,000 × *g* for 60 min at 4 °C. The pellets were resuspended in distilled water and centrifuged at 20,000 × *g* for 20 min at 4 °C. After resuspending the pellets in distilled water, the flagellin preparations were stored at −80 °C.

H_2O_2 Detection and Quantification—H_2O_2 produced in the medium of cultured cells was monitored based on chemiluminescence due to the ferricyanide-catalyzed oxidation of luminol (5-amino-2,3 dihydro-1,4-phthalazinedione) as described by Schwacke and Hager (24). Ten milligrams of cultured cells were transferred to 1 ml of fresh medium and preincubated for 2 h at 30 °C. Cultured rice cells were incubated with each flagellin (<100 μl) at 30 °C for the indicated periods after treatment. Following this incubation, 10 μl of the medium were harvested; added to 160 μl of 50 mM potassium phosphate buffer (pH 7.9), 10 μl of 1.1 mM luminol, and 20 μl of 14 mM potassium ferricyanide; and immediately analyzed for chemiluminescence using a Genelight55 Lumi-Counter (Microtec Co., Ltd., Chiba, Japan).

Quantitative Real Time RT-PCR—Total RNA was isolated from cultured rice cells using an RNeasy Plant Mini kit (Qiagen, Hilden, Germany) with DNase digestion according to the manufacturer's instructions. Quantitative real time RT-PCR was performed on an Opticon2 instrument (Bio-Rad) using a QuantiTect SYBR Green RT-PCR kit (Qiagen) with *PAL* gene-specific primers (forward, 5′-ACATCTACGGCGTCACCAC-3′; reverse, 5′-GAAGATTCCGGCGTTGAG-3′) and *Cht-1* gene-specific primers (forward, 5′-TTCTACACCTACGACGCCTTC-3′; reverse, 5′-TGGTCTCGTGCGACGTCTG-3′). To eliminate DNA contamination during quantitative RT-PCR, the primer set was designed across an intron. The sizes of the PCR products were examined to confirm that only mRNA was amplified in all quantitative RT-PCR experiments. The fluorescence data produced sigmoidal amplification plots in which the number of cycles was plotted against the fluorescence. The *PAL* and *Cht-1* mRNA levels were calculated using a calibration curve that was prepared using standard *PAL* and *Cht-1* genes of known template amounts (1 ng–0.1 pg) and normalized based on the reference gene *Act-1*.

Mass Spectrometry—All mass spectra were obtained on a Voyager™ Workstation MALDI-TOF mass spectrometer (Applied Biosystems, Foster City, CA) in a linear, positive mode. The sample solutions were prepared in water containing 0.1% TFA. All samples were prepared by a dried droplet method in which the analyte (intact protein or peptide mixture) was mixed with a 2.3-fold volume of matrix solution (a saturated solution of sinapinic acid in 100% acetonitrile with 0.1% TFA (v/v)), and then the mixture was deposited on a stainless target plate. To prepare for the peptide mass measurements, the monomeric flagellin proteins were incubated at 37 °C overnight with trypsin (Roche Applied Science) (protein:trypsin, 1:5 (w/w) in 50 mM NH_4HCO_3).

Detection of Glycoproteins—The flagellin concentration was determined with a protein assay kit (Bio-Rad) using BSA as the standard. Five micrograms of each purified flagellin were separated by SDS-polyacrylamide gel electrophoresis (PAGE) (10%, v/v). After SDS-PAGE, the glycoproteins were detected using a GelCode glycoprotein detection kit (Pierce) according to the manufacturer's instructions.

Generation of Fgt and FlaA Deletion Mutants—N1141 and K1 cosmid libraries were screened using an *FlaA*-specific probe for identification of *Fgt* genes. Two cosmid clones, N1141-10C6 and K1-12A11, were selected as *FlaA*-containing clones. Double-stranded sequences were aligned and assembled by using programs in the Genetyx software (Genetyx Co., Ltd., Tokyo, Japan). *NFgt* and *KFgt* were located in the 1.5-kbp upstream region of *FlaA*. *Fgt* and *FlaA* deletion mutants for the K1 and N1141 strains were generated using homologous recombination. For the *Fgt* deletion mutants of the K1 and N1141 strains, ~6-kbp DNA fragments containing the *N* or *KFgt* genes were PCR-amplified using two sets of specific primers (5′-GCCCAGGATGGTGACGATCTCGAA-3′ and 5′-CCAACTGGAACAACTGCATGACCA-3′ and 5′-TCTAGAGAGAAGAAGACCCCGAAGAT-3′ and 5′-ACTTCCCGCTGCTCAGCCTG-3′, respectively). Amplified fragments were cloned into the pCR2.1 TOPO vector (Invitrogen). The resulting plasmids, pN6F (for the N1141 *Fgt* deletion mutant) and pK6F (for the K1 *Fgt* deletion mutant), were digested with SmaI and SacII, respectively, and then self-ligated to remove the 2-kbp mutation sites. The resulting plasmid, pN4F (for the N1141 *Fgt* deletion mutant), was digested with EcoRI and BglII and then cloned into the pK18*mobsacB* vector (25). pK5F (for the K1 *Fgt* deletion mutant) was also digested with XbaI and cloned into pK18*mobsacB*. The resulting plasmids, designated pNΔ*Fgt* and pKΔ*Fgt*, were electrotransformed into the *A. avenae* N1141 and K1 strains, respectively. After transformation, the bacterial cells were plated on LB agar plates containing 20 μg/ml kanamycin and incubated for 48 h at 30 °C. The resulting colonies were inoculated into *Pseudomonas* F liquid medium containing 26% sucrose and incubated for 72 h at 30 °C to excise the plasmid by a second crossover event. The resulting bacteria were designated *N*Δ*Fgt* and *K*Δ*Fgt*. To generate the *FlaA* deletion mutants, ~1-kbp DNA fragments located on each side of *FlaA* were PCR-amplified using two sets of specific primers (5′-TCTAGATAGTGTTCTCGCCCTTGACCG-3′ and 5′-GGATCCTGCCATTGCAAATCTCCTGAA-3′ for the upstream region of N1141 *FlaA* and 5′-GGATCCCGTTGATTGCGCAGGGCTG-3′ and 5′-TCTAGAAACGCGCTGTTGACGGCGTTG-3′ for the downstream region of N1141 *FlaA*; 5′-TCTAGAATGCCGTGCTGTTCTCACCCTTG-3′ and 5′-GGATCCTGCCATTGCAAATCTCCTGAA-3′ for the upstream region of K1 *FlaA* and 5′-GGATCCCGTTGATGTCGCAGGGCTGAA-3′ and 5′-TCTAGACGTCTTCGTGTCCTTGTCGTACTTC-3′ for the downstream region of K1 *FlaA*). Each amplified DNA fragment was cloned into the pGEM-T vector (Promega, Corp., Madison, WI), and the resulting plasmids, pNU and pND as well as pKU and pKD, were digested with BamHI and NotI. The digested upstream fragment and downstream fragment were ligated and cloned into the pGEM-T vector. The resulting plasmids, pNUD containing DNA fragments lacking *NFlaA* and pKUD containing DNA fragments lacking *KFlaA*, were digested with XbaI and then cloned into the pK18*mobsacB* vector. The resulting plasmids, designated pNΔ*FlaA* and pKΔ*FlaA*, were electrotransformed into the *A. avenae* N1141 and K1 strains, respectively. After transformation, the bacterial cells were plated on LB agar plates containing 20 μg/ml kanamycin and incubated for 48 h at 30 °C. The resulting colonies were inoculated into *Pseudomonas* F liquid medium containing 26% sucrose and incubated for 72 h at 30 °C to excise the plasmid through a second crossover event. The resulting bacteria were designated *N*Δ*FlaA* and *K*Δ*FlaA* (Table 1). For the swimming assay, each bacterial cell was inoculated onto 0.25% agar LB plates with a needle and incubated for 24 h at 30 °C.

Generation of Flagellins with Amino Acid Substitutions—To generate the amino acid-substituted flagellins, a KOD-Plus mutagenesis kit (Toyobo, Osaka, Japan) was used. An ~2-kbp DNA fragment containing the region from 231 bp upstream to 299 bp downstream of *KFlaA* was PCR-amplified with a specific primer set (5′-CCCGGGGCATTGGGGGGATAA-3′ and 5′-AAGCTTGACGGCATCCACGGCAG-3′) and cloned into the pGEM-T vector. This double-stranded plasmid vector was used as a template to generate mutant flagellins. The DNA for each *KFlaA* mutant was reverse amplified using the following PCR primer sets containing the noted mutations: K S178A, 5′-GCTGGCGCGGCTACCTCCGGCG-3′ and 5′-GGCCGAGGCCGTCAGTTGGGCGC; K S183A, 5′-GCTGGCGCGTCGGCCGGCTCG-3′ and 5′-GGTAGCCGCGCCGGAGGCCGAG-3′; K S212A, 5′-GCTGGCACGGCCGCCGACATC-3′ and 5′-GGCGGCGACGTTGACGGTCTTG-3′; K T351A, 5′-GCCGGTGCCACCGTGGCCTCG-3′ and 5′-GCCCGCCGCCGTGGCGGT-3′; and K S178A/S183A, 5′-GCTGGCGCGTCGGCCGGCTCG-3′ and 5′-GGTAGCCGCGCCAGCGGCCGAG-3′. The desired mutations were confirmed by DNA sequence analysis, and the plasmids were digested with SmaI and HindIII. For each mutant, a DNA fragment of ~2 kbp was isolated and ligated into the SmaI and HindIII digestion sites within the pKΔ*FlaA* vector. The resulting plasmids were digested with XbaI and then inserted into the pK18*mobsacB* vector. The resulting plasmids were transformed into the *A. avenae* N1141 or K1 strain. After transformation, the bacterial cells were plated on LB agar plates containing 20 μg/ml kanamycin and incubated for 48 h at 30 °C. The colonies were inoculated into *Pseudomonas* F liquid medium containing 26% sucrose and incubated for 72 h at 30 °C to excise the plasmid by a second crossover event. The resulting bacteria were designated K1-^{178}Ser/Ala, K1-^{183}Ser/Ala, K1-^{212}Ser/Ala, K1-^{351}Thr/Ala, and K1-^{178}Ser/Ala ^{183}Ser/Ala, respectively. Mutants (designated K1-^{178,183,212,351}Ala) with four substitutions (K1-S178A/S183A/S212A/T351A) were also generated using the same method (Table 1).

Electron Microscopy—For negative staining, 50-μl droplets of the sample solution were used. Samples were allowed to absorb for 1 min onto collodion-coated grids supported with carbon, which rendered the carbon surface hydrophilic. The grids were stained for 1 min with 1% (w/v) phosphotungstic acid (pH 6.9) (Merck) and washed with two drops of distilled water. Images were taken as digitized pictures with a Hitachi

TABLE 1
Bacterial strains and plasmids used in this study
Km^r, kanamycin resistance.

Bacterial strains and plasmids	Relevant characteristic	Ref. or source
Strains		
E. coli		
DH5a	F$^-$λ$^-$ *ϕ80dLacZΔM15* Δ(*lacZYA-argF*)*U169 recA1 endA1 hsdR17*(*rK*$^-$*mK*$^+$) *supE44 thi-1 gyrA relA1*	Takara, Kyoto, Japan
A. avenae		
N1141	Wild type	Che *et al.* (21)
NΔFgt	N1141 mutant; Δ*Fgt*	This study
NΔFlaA	N1141 mutant; Δ*FlaA*	This study
NΔFlaA-NFlaA	N1141 mutant; *NFlaA*	This study
NΔFlaA-KFlaA	N1141 mutant; *KFlaA*	This study
K1	Wild type	Che *et al.* (21)
KΔFgt	K1 mutant; Δ*Fgt*	This study
KΔFlaA	K1 mutant; Δ*FlaA*	This study
KΔFlaA-KFlaA	K1 mutant; *KFlaA*	This study
KΔFlaA-NFlaA	K1 mutant; *NFlaA*	This study
K1-^{178}Ser/Ala	K1 mutant; S178A	This study
K1-^{183}Ser/Ala	K1 mutant; S183A	This study
K1-^{212}Ser/Ala	K1 mutant; S212A	This study
K1-^{351}Thr/Ala	K1 mutant; T351A	This study
K1-^{178}Ser/Ala ^{183}Ser/Ala	K1 mutant; S178A/S183A	This study
K1-^{178,183,212,351}Ala	K1 mutant; S178A/S183A/S212A/T351A	This study
Plasmids		
pK18*mobsacB*	Sucrose-sensitive (sacB) Km^r	Schäfer *et al.* (25)
pNΔ*Fgt*	4-kb chimeric PCR product mutating *NFgt* cloned into pK18*mobsacB* at EcoRI and BglII sites, Km^r	This study
pKΔ*Fgt*	5-kb chimeric PCR product mutating *KFgt* cloned into pK18*mobsacB* at XbaI site, Km^r	This study
pNΔ*FlaA*	2.1-kb chimeric PCR product deleting *NFlaA* cloned into pK18*mobsacB* at XbaI site, Km^r	This study
pKΔ*FlaA*	2.2-kb chimeric PCR product deleting *KFlaA* cloned into pK18*mobsacB* at XbaI site, Km^r	This study

H-7100 transmission electron microscope operated at 80 kV using a 2K charge-coupled device camera (XR-41, Advanced Microscopy Technique Corp.)

RESULTS

Induction of Immune Responses by Recombinant Flagellins Produced in E. coli—We previously reported that rice immune responses are induced by flagellin from the rice avirulent N1141 strain but not by flagellin from the rice virulent K1 and H8301 strains. Furthermore, the flagellins of the N1141 and K1 strains are composed of 492 amino acids with only 14 residues differing between these flagellins (21). To determine whether these differences in the amino acid sequences between the N1141 and K1 flagellins primarily cause the specific immune responses in rice cells, His-tagged N1141 and K1 flagellins were produced in *E. coli* and purified using HisTrap affinity chromatography. The MALDI-TOF mass spectrum of the purified recombinant N1141 and K1 flagellins showed that the recombinant N1141 flagellin had a molecular mass of 50,450 Da, whereas recombinant K1 flagellin had a mass of 50,310 Da (data not shown). The measured masses of the recombinant N1141 and K1 flagellins are highly similar to the calculated molecular masses (50,454 and 50,309 Da, respectively), suggesting that the N1141 and K1 flagellins are not modified. To clarify the role of the amino acids that differ between the N1141 and K1 flagellins in the specific induction of immune responses, H_2O_2 generation was examined as a readout for the plant immune responses using a luminol chemiluminescence assay (24). When N1141 flagellin was added to cultured rice cells, H_2O_2 was rapidly generated within 60 min after treatment, and the ratio of H_2O_2 generation gradually decreased until 3 h after treatment. In contrast, K1 flagellin did not cause a detectable increase in H_2O_2 generation until 3 h after treatment (Fig. 1*A*). When cultured rice cells were treated with the recombinant His-tagged N1141 flagellins, H_2O_2 was rapidly generated as observed with the purified N1141 flagellin. Interestingly, the recombinant His-tagged K1 flagellin also caused rapid H_2O_2 generation in cultured rice cells to the same degree as the recombinant N1141 flagellin (Fig. 1*B*).

We have reported that expression of *PAL*, which encodes phenylalanine ammonia-lyase and catalyzes the first step in the biosynthesis of lignin monomers and certain classes of phytoalexins, was increased upon the addition of purified N1141 flagellin but not purified K1 flagellin (20). To clarify whether the N1141 flagellin-specific induction of the *PAL* gene depends on the amino acid residues that are different between the N1141 and K1 flagellins, quantitative real time RT-PCR was performed using the purified and recombinant flagellins. Purified N1141 and K1 flagellins were added to cultured rice cells, and total RNA was extracted after 0, 1, 3, and 6 h. *PAL* transcripts were induced 1 h after inoculation with the flagellin purified from the N1141 strain, and the expression levels gradually increased up to 6 h, whereas *PAL* mRNA did not increase upon treatment with the flagellin purified from the K1 strain (Fig. 1*C*). In contrast, when the recombinant flagellins were used for this experiment, the *PAL* mRNA levels increased not only with the N1141 recombinant flagellin but also with the K1 recombinant flagellin. Thus, the increased *PAL* mRNA levels together with the comparable H_2O_2 generation showed that the specific induction of immune responses between N1141 and K1 flagellins did not depend on the amino acids that differ between these flagellins.

Identification of Flagellin Glycosylation Genes—Because the amino acid substitutions between N1141 and K1 flagellins did not regulate the induction specificity of the rice immune response, we assumed that post-translational modification(s) of these flagellins is involved in the specificity of the immune responses. We reported that flagellins of the *A. avenae* N1141 and K1 strains were glycosylated and that the glycans differed between N1141 flagellin and K1 flagellin (21). Therefore, we

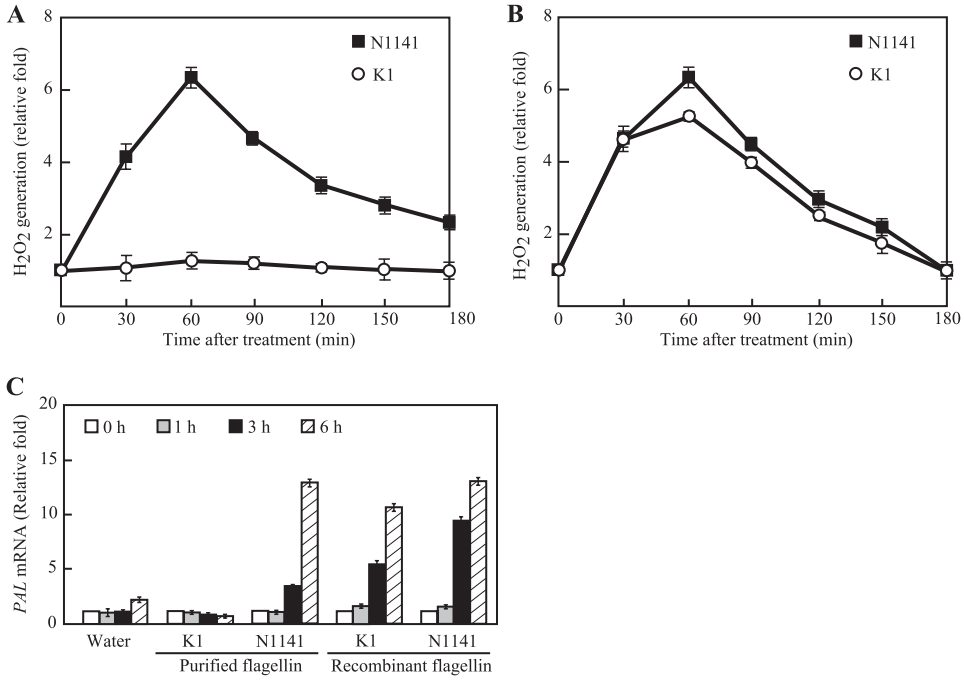

FIGURE 1. **Induction of immune responses in cultured rice cells by flagellin from *A. avenae*.** *A*, time course of H_2O_2 generation in cultured rice cells that were treated with flagellin purified from the avirulent N1141 strain (*solid squares*) or virulent K1 strain (*open circles*). The *y axis* represents the -fold change in H_2O_2 in cultured rice cells relative to the levels before flagellin treatment. *B*, time course of H_2O_2 generation in cultured rice cells treated with recombinant flagellin from the avirulent N1141 strain (*solid squares*) or virulent K1 strain (*open circles*) produced in *E. coli*. H_2O_2 was detected using a luminol chemiluminescence assay. The *y axis* represents the -fold change in H_2O_2 in cultured rice cells relative to the levels before flagellin treatment. *C*, *PAL* mRNA levels in cultured rice cells that were treated with flagellin purified from the N1141 or K1 strain and recombinant flagellin of the N1141 or K1 strain. The mRNA levels were calculated from the threshold point located in the log-linear range of RT-PCR. Standard samples with known template amounts were used to quantitate the *PAL* mRNA levels. The *y axis* represents the -fold change in *PAL* mRNA levels relative to the levels in water-treated cultured rice cells. *White columns*, 0 h after treatment; *gray columns*, 1 h after treatment; *black columns*, 3 h after treatment; *hatched columns*, 6 h after treatment. The *error bars* in all figures indicate the S.D. for five experiments.

next clarified whether the glycosylation of flagellins in *A. avenae* affects the induction specificity of the immune response in rice cells.

The N1141 and K1 flagellin sequences showed no evidence of a classic eukaryotic *N*-linked sequence or the more recently defined prokaryotic *N*-linked consensus sequences, suggesting that the glycan was *O*-linked (26). The glycan was removed from the flagellins by chemical degradation or enzymatic digestion. However, these trials were not successful because the flagellin proteins were degraded or aggregated by these treatments (data not shown). It was reported that the glycosyltransferase gene within the flagellar gene operon of *Pseudomonas aeruginosa* or *Pseudomonas syringae* is necessary for flagellin glycosylation and that deleting this gene results in the production of non-glycosylated flagellin (27, 28). Therefore, we next identified the glycosyltransferase gene within the flagellar operon in the *A. avenae* N1141 and K1 strains. Genomic clones from DNA cosmid libraries of the N1141 and K1 strains were screened using the PCR product for each *FlaA* gene that encodes flagellin (21) as a DNA probe, and then the nucleotide sequences upstream of *FlaA* were determined. The sequence analysis of the region upstream of the N1141 and K1 strains showed that putative glycosyltransferase genes, designated *NFgt* and *KFgt*, were located near the flagellar motor gene *MotA*, which is located in the 1.5-kbp upstream region of *FlaA* (supplemental Fig. 2). *NFgt* contained an open reading frame of 4,077 bp that encoded a 1,359-amino acid protein with a calculated molecular weight of 150,768. *KFgt* is composed of 3,795 bp and is predicted to encode a protein of 1,265 amino acids with a calculated molecular weight of 139,780. The deduced amino acid sequences showed that the sequence identity between these N1141 and K1 glycosyltransferases is relatively low (61%).

Generation Fgt and FlaA Deletion Mutants—To examine whether the *NFgt* and *KFgt* genes are responsible for flagellin glycosylation in *A. avenae*, we generated *Fgt* deletion mutants and *FlaA* deletion mutants using homologous recombination. The regions up- and downstream of each gene were PCR-amplified from N1141 and K1 genomic DNA. The purified products were joined and then ligated into the pK18*mobsacB* plasmid. Isogenic *A. avenae* N1141 and K1 mutants were made in each corresponding pK18*mobsacB* plasmid. Two *Fgt* deletion mutants, designated *N*Δ*Fgt* (from N1141) and *K*Δ*Fgt* (from K1), and two *FlaA* deletion mutants, designated *N*Δ*FlaA* and *K*Δ*FlaA*, were generated.

All mutant strains had normal viability and growth. The motility of the four mutants was examined based on a swimming assay on soft agar plates. For the *N*Δ*FlaA* and *K*Δ*FlaA* strains in which the *FlaA* gene was deleted, the cells were completely non-motile as demonstrated by the small, sharply delineated colonies that are typical of non-motile cells on soft agar (Fig. 2*A*). In contrast, the *N*Δ*Fgt* and *K*Δ*Fgt* strains had a diffuse spreading growth pattern that is characteristic of motile bacteria and that was similar to the parental strains (Fig. 2*A*). The morphological features of the *N*Δ*Fgt* and *K*Δ*Fgt* strains were observed by transmission electron microscopy using negative staining and compared with the parental strains. These

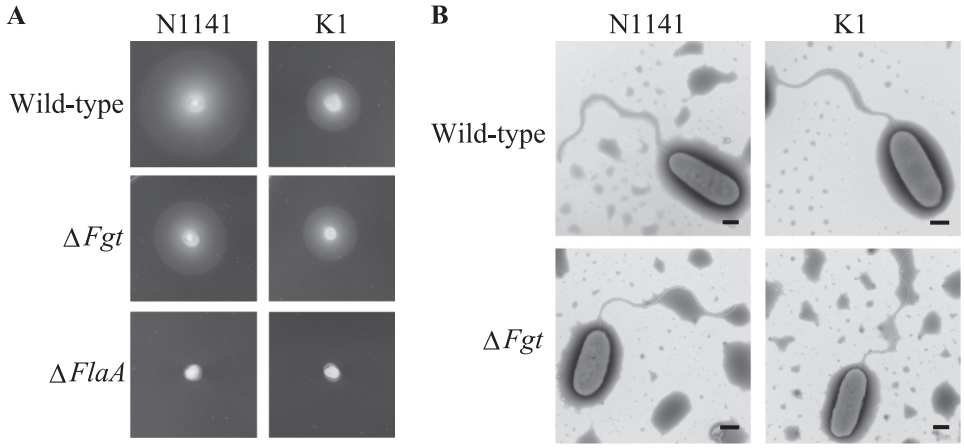

FIGURE 2. **Functions of *FlaA* and *Fgt* genes in *A. avenae* N1141 and K1 strains.** *A*, swimming motility of the wild-type, Δ*Fgt*, and Δ*FlaA* strains of *A. avenae*. Bacterial cell densities were adjusted to an A_{610} of 1.0, and 2-μl aliquots were inoculated on LB soft agar plates. Photographs were taken after 24 h at 30 °C. *B*, transmission electron micrograph of wild-type and Δ*Fgt* strains of *A. avenae* N1141 and K1. The *bars* represent 500 nm.

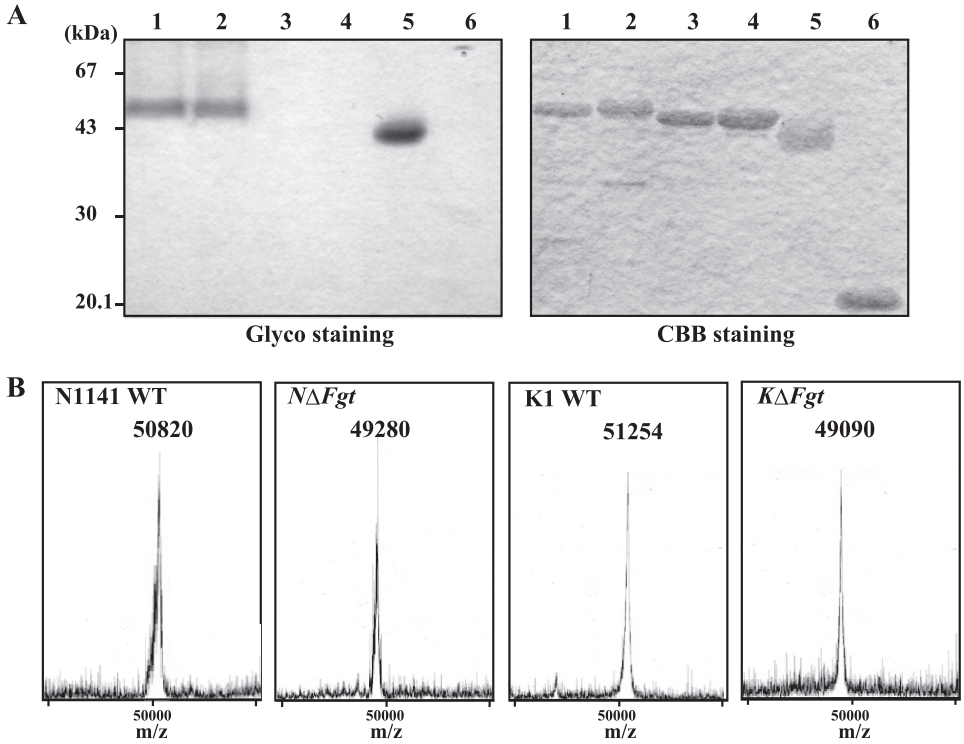

FIGURE 3. **Structural analysis of flagellin purified from N1141 wild-type, N1141 Δ*Fgt*, K1 wild-type, and K1 Δ*Fgt* strains of *A. avenae*.** *A*, detection of sugar moieties in the N1141 wild-type, N1141 Δ*Fgt*, K1 wild-type, and K1 Δ*Fgt* flagellins of *A. avenae*. SDS-PAGE and Coomassie Brilliant Blue R-250 (*CBB*) (*right*) or glycoprotein (*Glyco*) staining (*left*) are shown. *Lane 1*, flagellin of the N1141 wild-type strain; *lane 2*, flagellin of K1 wild-type strain; *lane 3*, flagellin of the N1141 Δ*Fgt* strain; *lane 4*, flagellin of the K1 Δ*Fgt* strain; *lane 5*, horseradish peroxidase (positive control); *lane 6*, soybean trypsin inhibitor (negative control). Five micrograms of protein were loaded into each lane, and a prestained protein marker was used to identify the molecular weights. *B*, MALDI-TOF MS analysis of flagellins purified from the N1141 wild-type (*N1141 WT*), N1141 Δ*Fgt* (*N*Δ*Fgt*), K1 wild-type (*K1 WT*), and K1 Δ*Fgt* (*K*Δ*Fgt*) strains of *A. avenae*. The molecular ion peaks obtained by MALDI-TOF MS analyses showed that molecular weights of flagellins purified from the N1141 wild-type, N1141 Δ*Fgt*, K1 wild-type, and K1 Δ*Fgt* strains of *A. avenae* are ~50,820, 49,280, 51,254, and 49,090, respectively.

were characteristic polar flagella on the *N*Δ*Fgt* and *K*Δ*Fgt* strains, and the length and diameter of the flagella on the *N*Δ*Fgt* and *K*Δ*Fgt* strains were very similar to those of the parental cells (Fig. 2*B*).

*Characterization of Deglycosylated Flagellins in N*Δ*Fgt and K*Δ*Fgt Strains*—To analyze the effects of deleting the glycosyltransferase genes on the sugar chain of each flagellin, the flagellins were separated by SDS-PAGE and stained using a glycoside detection kit (Pierce). SDS-PAGE and subsequent Coomassie Brilliant Blue R-250 staining showed that the flagellin protein from the *N*Δ*Fgt* mutant migrated at a position that was ~1.5 kDa smaller than the protein from the wild-type N1141 strain. Furthermore, the flagellin protein from *K*Δ*Fgt* was ~2 kDa smaller than that of the flagellin protein from the wild-type K1 strain. When the flagellin proteins were separated by SDS-PAGE and stained with a glycoside detection kit, the N1141 and K1 wild-type flagellins and horseradish peroxidase (as a positive glycosylated protein control) were stained (Fig. 3*A*). In contrast,

the *NΔFgt* and *KΔFgt* flagellins and the soybean trypsin inhibitor (as a non-glycosylated protein control) could not be detected using this staining method (Fig. 3*A*), suggesting that the flagellin proteins of the *NΔFgt* and *KΔFgt* strains were deglycosylated.

To determine the molecular mass of the sugar chains in the flagellin proteins, MALDI-TOF MS analysis was performed. The mass spectrum of the N1141 wild-type flagellin showed that the molecular mass of the mature-type N1141 flagellin is 50,820 Da, which is greater than the calculated molecular mass by ~1,600 Da. The molecular mass of K1 flagellin is 51,254 Da, which is also greater than the calculated molecular mass by ~2,150 Da (Fig. 3*B*). Mass spectrometry analysis also showed that the molecular masses of the *NΔFgt* and *KΔFgt* flagellins are 49,280 and 49,090 Da, respectively, which are highly similar to the respective calculated masses (Fig. 3*B*). The mass spectrum data together with the mobility shift in the SDS-PAGE analysis revealed that no glycans are present on the flagellins from the *NΔFgt* and *KΔFgt* strains.

Function of Flagellin Glycosylation in Induction of Immune Responses in Rice—To clarify the specific induction mechanism by *A. avenae* flagellin in rice cells, the ability of the deglycosylated flagellins to induce H_2O_2 was measured. When the flagellin purified from the *NΔFgt* strain was added to cultured rice cells, H_2O_2 was rapidly generated within 60 min after treatment, and the ratio of H_2O_2 generation gradually decreased until 3 h after treatment. The same pattern of H_2O_2 generation was observed with the N1141 mature-type flagellin purified from the N1141 wild-type strain (Fig. 4*A*). Interestingly, when the cultured rice cells were treated with the deglycosylated flagellin from *KΔFgt*, H_2O_2 was rapidly generated, whereas the K1 mature-type flagellin purified from the K1 wild-type strain did not cause a detectable increase in H_2O_2 until 3 h after treatment (Fig. 4*B*). Additionally, the H_2O_2 patterns generated by the deglycosylated K1 flagellin and N1141 flagellin were consistent.

Induction of *PAL* gene expression was also examined by quantitative real time RT-PCR (Fig. 4*C*). *PAL* transcripts were induced 1 h after treatment with N1141 flagellin and the deglycosylated N1141 flagellin, and these expression levels gradually increased up to 6 h after treatment. In contrast, the *PAL* mRNA levels did not increase upon treatment with K1 flagellin, whereas the K1 deglycosylated flagellin purified from *KΔFgt* induced *PAL* mRNA but to a lesser extent compared with the levels measured in response to N1141 flagellin (Fig. 4*C*). These data suggest that deglycosylation determines the ability of K1 flagellin to induce immune responses.

To clarify whether the characteristic glycan form and the attachment site in each bacterial strain of *A. avenae* are involved in the specific induction of rice immune responses, each N1141 *FlaA* and K1 *FlaA* expression vector was introduced into the *NΔFlaA* and *KΔFlaA* strains, and the flagellin was purified from each bacterial strain. The K1-type flagellin purified from the *KΔFlaA-KFlaA* strain did not induce H_2O_2 in the same manner as the K1 wild-type flagellin, whereas the K1-type flagellin purified from the *NΔFlaA-KFlaA* strain rapidly induced H_2O_2 that continued for 90 min after treatment (Fig. 4*D*). In contrast, when the N1141-type flagellin that was purified from the *KΔFlaA-NFlaA* strain was added to cultured rice cells, there was no observable H_2O_2, whereas the flagellin from the *NΔFlaA-NFlaA* strain caused rapid H_2O_2 generation in the same manner as the N1141 wild-type flagellin (Fig. 4*E*). Furthermore, *PAL* gene expression was also induced by flagellins purified from the *NΔFlaA-NFlaA* and *NΔFlaA-KFlaA* strains, whereas no induction of *PAL* mRNA was observed when cultured rice cells were treated with the flagellin purified from the *KΔFlaA-KFlaA* and *KΔFlaA-NFlaA* strains (Fig. 4*F*). These data together with the data of H_2O_2 induction clearly indicate that the characteristic glycan form or glycan attachment site in the K1 strain contributes to flagellin recognition by rice.

Determination of Glycan Attachment Site in K1 Flagellin—The induction specificity of the rice immune responses observed between the N1141 and K1 flagellins depended on the glycan form and attachment sites in K1 flagellin. Therefore, we next examined the exact glycan attachment sites and characterized the glycans in K1 flagellin. To determine the exact sites of glycan attachment, the flagellins purified from the K1 and *KΔFgt* strains were digested with trypsin, and the molecular mass of each digested peptide was measured by mass spectrometry. Three peaks were detected as specific fragments that differed between the K1 and *KΔFgt* strains. Three sharp peaks were observed at *m*/*z* 2,822, 3,527, and 5,963 in the *KΔFgt* flagellin digestion mixtures, whereas ion peaks of *m*/*z* 3,362, 4,607, and 6,503 were detected in K1 flagellin digestion mixtures (Fig. 5). A prediction analysis of tryptic peptides from *KΔFgt* flagellin revealed that the obtained ion peaks at *m*/*z* 2,822, 3,527, and 5,963 could be readily assigned as Thr^{206}–Arg^{236} (expected molecular mass, 2,821 Da), Thr^{166}–Lys^{205} (expected molecular mass, 3,526 Da), and Leu^{296}–Arg^{358} (expected molecular mass, 5,962 Da), respectively. In contrast, three specific peaks in the tryptic K1 flagellin did not match any expected tryptic peptides, suggesting that a glycan was attached to the three fragments of K1 flagellin, Thr^{206}–Arg^{236}, Thr^{166}–Lys^{205}, and Leu^{296}–Arg^{358}. In each case, the molecular mass difference in each peak of the tryptic *KΔFgt* flagellin and corresponding peak for the tryptic K1 flagellin was ~540 Da (Thr^{206}–Arg^{236}), 1,080 (Thr^{166}–Lys^{205}), and 540 (Leu^{296}–Arg^{358}). Because the molecular mass difference in the Thr^{166}–Lys^{205} fragments between K1 and *KΔFgt* flagellin is a multiple of that of Thr^{206}–Arg^{236} or Leu^{296}–Arg^{358}, the same two glycans may be present in the Thr^{166}–Lys^{205} fragment of K1 flagellin. In addition, the 51,254-Da molecular mass of intact K1 flagellin determined by mass spectrometry was 2,164 Da larger than that predicted from the K1 flagellin sequence or that of *KΔFgt* (Fig. 3*B*), suggesting that glycans were attached to all three fragments of K1 flagellin.

Identification of Glycosylated Residues in K1 Flagellin of A. avenae—To determine the location of the attached glycan, purified flagellin proteins from the *KΔFgt* and K1 strains were digested with trypsin and aspartic *N*-peptidase and then analyzed by reverse-phase HPLC. As shown in Fig. 6*A*, a comparison of the retention times of the peptide fragments produced by the digestion revealed one specific peak (retention time of 38 min) only in the chromatogram for K1 flagellin. N-terminal sequencing analysis revealed that this fragment corresponded

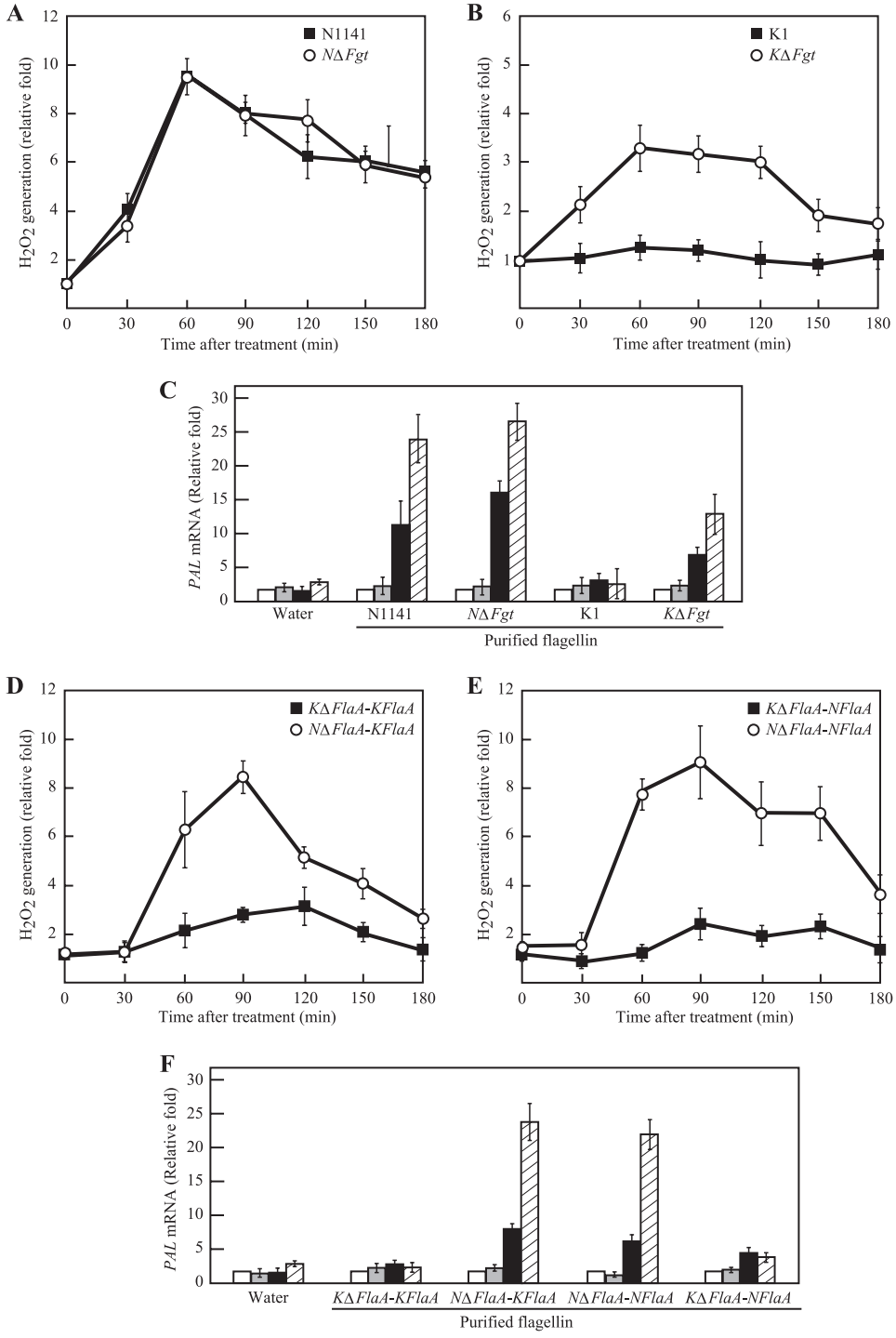

FIGURE 4. **Induction of immune responses in cultured rice cells by flagellins purified from N1141 wild-type, N1141 Δ*Fgt*, K1 wild-type, and K1 Δ*Fgt* strains of *A. avenae*.** *A*, time course of H_2O_2 generation in cultured rice cells that were treated with flagellin purified from the N1141 wild-type (*solid squares*) or N1141 Δ*Fgt* (*open circles*) strain. *B*, time course of H_2O_2 generation in cultured rice cells that were treated with flagellin purified from the K1 wild-type strain (*solid squares*) or K1 Δ*Fgt* (*open circles*) strain. H_2O_2 was detected using a luminol chemiluminescence assay. *C*, *PAL* mRNA levels in cultured rice cells that were treated with flagellins purified from the N1141 wild-type, N1141 Δ*Fgt*, K1 wild-type, and K1 Δ*Fgt* strains of *A. avenae*. The mRNA levels were calculated from the threshold point located in the log-linear range of RT-PCR. Standard samples with known template amounts were used to quantitate the *PAL* mRNA levels. The *y axis* represents the -fold change relative to the *PAL* mRNA levels of water-treated cultured rice cells. *White columns*, 0 h after treatment; *gray columns*, 1 h after treatment; *black columns*, 3 h after treatment; *hatched columns*, 6 h after treatment. *D*, time course of H_2O_2 generation in cultured rice cells that were treated with K1-type flagellin purified from the *KΔFlaA-KFlaA* (*KΔFlaA* strain carrying the K1 *FlaA* expression vector) (*solid squares*) or *NΔFlaA-KFlaA* (*NΔFlaA* strain carrying the K1 *FlaA* expression vector) (*open circles*) strain. *E*, time course of H_2O_2 generation in cultured rice cells that were treated with N1141-type flagellins purified from the *KΔFlaA-NFlaA* (*KΔFlaA* strain carrying the N1141 *FlaA* expression vector) (*solid squares*) or *NΔFlaA-NFlaA* (*NΔFlaA* strain carrying the N1141 *FlaA* expression vector) (*open circles*) strain. *F*, *PAL* mRNA levels in cultured rice cells that were treated with flagellins purified from the *KΔFlaA-KFlaA*, *NΔFlaA-KFlaA*, *NΔFlaA-NFlaA*, and *KΔFlaA-NFlaA* strains of *A. avenae*. The mRNA levels were calculated from the threshold point located in the log-linear range of RT-PCR. Standard samples with known template amounts were used to quantitate the *PAL* mRNA levels. The *y axis* represents the -fold change relative to the *PAL* mRNA levels of water-treated cultured rice cells. *White columns*, 0 h after treatment; *gray columns*, 1 h after treatment; *black columns*, 3 h after treatment; *hatched columns*, 6 h after treatment. The *error bars* in all figures indicate the S.D. for five experiments.

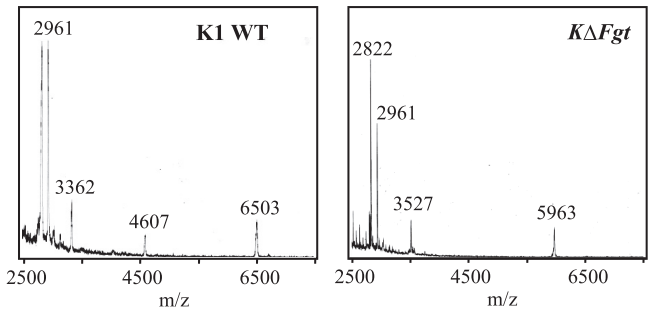

FIGURE 5. **MALDI-TOF MS analysis of trypsin-digested K1 wild-type flagellin (*left*) and K1 deglycosylated flagellin (*right*).** *K1 WT*, K1 wild-type flagellin; *KΔFgt*, K1 Δ*Fgt* flagellin. Each flagellin was digested with trypsin at 37 °C, and the mass spectra of the mixed flagellin digested peptides were measured using a Voyager Workstation MALDI-TOF mass spectrometer (Applied Biosystems) in a linear, positive mode with sinapinic acid as the matrix.

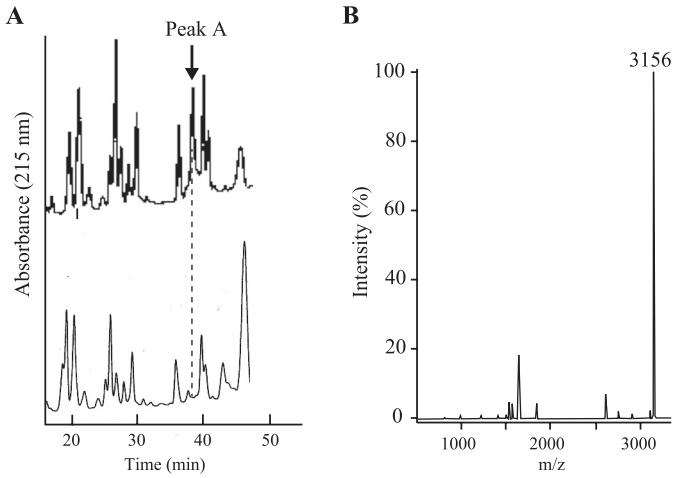

FIGURE 6. **Detection of amino acids harboring glycan attachment site in flagellin from *A. avenae* K1 strain.** *A*, HPLC chromatograms of a flagellin fragment derived from trypsin and aspartic *N*-peptidase digestion of each flagellin. After digesting K1 wild-type flagellin (*upper* chromatogram) and K1 Δ*Fgt* flagellin (*lower* chromatogram) with trypsin and aspartic *N*-peptidase, the peptide fragments were detected by reverse-phase HPLC as described under "Experimental Procedures." Peak A was detected only in the chromatogram for the K1 wild-type flagellin. The *bottom* amino acid sequence represents the amino acid sequence of peak A obtained with N-terminal sequencing analysis using a peptide sequencer (Applied Biosystems 492cLC). The *X* residue in the amino acid sequence for peak A (*bottom*) indicates an amino acid residue that was not identified in the N-terminal sequencing analysis. *B*, mass spectrum of peak A. The molecular mass ion 3,156 is 540 larger than that predicted from the peak A fragment.

to Asp^{331}–Arg^{358}. In this sequencing analysis, the Thr^{351} residue was not identified due to incorrect retention times, suggesting that this threonine residue is likely modified (Fig. 6*A*). MALDI-TOF MS analysis showed that the molecular mass of the fragment is 3,156 Da, which is 540 Da larger than the mass predicted based on the fragment sequence (Fig. 6*B*). These data indicated that a glycan with a molecular weight of ~540 may be attached to Thr^{351} in K1 flagellin.

In the HPLC analysis of the digested K1 and *KΔFgt* flagellins, we did not detect specific peaks with the exception of a peak consistent with Asp^{331}–Arg^{358}. Therefore, the other glycosylated residues were identified by performing site-directed mutagenesis of candidate glycosylated residues within the Thr^{166}–Lys^{205} and Thr^{206}–Arg^{236} fragments of K1 flagellin. A comparison of the amino acid sequences between K1 and N1141 flagellins showed that three amino acids (Ser^{178}, Ser^{183}, and Ser^{186}) and one amino acid (Ser^{212}) were substituted within the Thr^{166}–Lys^{205} and Thr^{206}–Arg^{236} fragments of K1 flagellin, respectively. Therefore, we assumed that these were primary candidates for glycosylated amino acid residues in K1 flagellin. Expression vectors encoding mutant flagellins in which the candidate serines were replaced with alanines were generated using the KOD-Plus mutagenesis kit and introduced into the K1 flagellin deletion mutant *KΔFlaA*. Each flagellin protein was purified from the corresponding mutant, and immunoblot analysis was performed using an anti-flagellin antibody. Monomeric flagellin proteins from single S178A, S183A, and S212A substitutions had a lower molecular mass than the K1 strain, whereas the molecular mass of the S186A mutant flagellin was not reduced (supplemental Fig. 1).

To confirm that the three serine residues in K1 flagellin were glycosylated, MALDI-TOF MS analyses were performed. The molecular masses of flagellins from the S178A, S183A, and S212A substituted mutants were ~1,616 Da larger than that predicted based on K1 flagellin, whereas the molecular mass of the S186A mutant flagellin was the same as that of K1 flagellin (Table 2). The Thr^{351} residue that is predicted to be attached to a glycan with a molecular weight of 540 was also replaced with an alanine residue. Consistent with our expectations, the molecular mass of the T351A mutant flagellin was ~540 Da lower than that of intact K1 flagellin (Table 2). These data suggest that the three serine residues at positions 178, 183, and 212 and the one threonine residue at position 351 in flagellin from the *A. avenae* K1 strain are glycosylated by glycans with molecular weights of approximately 540.

Induction of Immune Responses in Cultured Rice Cells by Flagellins with Mutated Glycan Attachment Site—Cultured rice cells that were treated with the S178A and S183A K1 flagellins produced higher levels of H_2O_2 than cells treated with K1 flagellin from the *KΔFlaA-KFlaA* strain 1 h after treatment, and the ratio of H_2O_2 generation gradually decreased until 3 h after treatment. The H_2O_2 generated by the S178A and S183A K1 substituted flagellins was similar to that induced by N1141 flagellin, and the ability of the S178A and S183A K1 substituted flagellins to stimulate H_2O_2 production was higher than that of N1141 flagellin from the *NΔFlaA-NFlaA* strain. Interestingly, the S178A/S183A K1 double substituted flagellin also induced H_2O_2 generation, and the ratio of H_2O_2 generation was similar to that induced by S178A K1 substituted flagellin. In contrast, the S212A and T351A K1 flagellins did not induce remarkable H_2O_2 generation until 3 h after treatment, which was the same as K1 flagellin from the *KΔFlaA-KFlaA* strain (Fig. 7*A*).

Induction of *PAL* gene expression by the substituted flagellins was also examined by quantitative real time RT-PCR (Fig. 7*B*). Induction of *PAL* mRNA expression was observed 6 h after treatment with the S178A and S183A K1 flagellins and S178A/S183A K1 double substituted K1 flagellin, whereas significant induction of *PAL* mRNA was not detected at 6 h after treatment with the S212A and T351A K1 flagellins, which was the same as K1 flagellin from the *KΔFlaA-KFlaA* strain.

Cht-1 encodes the chitinase enzyme, which hydrolyzes the β-1,4-linkage between *N*-acetyl-D-glucosamine residues of chi-

TABLE 2

Molecular masses of intact flagellin (Ala^2–Arg^{492}) and peptide fragments (Thr^{166}–Lys^{205}, Thr^{206}–Arg^{236}, and Leu^{296}–Arg^{358})

M, major molecular masses (in Da) measured by MALDI-TOF MS; P, molecular masses (in Da) predicted by deduced amino acid sequence.

	Intact (Ala^2–Arg^{492})			Fragment (Thr^{166}–Lys^{205})		Fragment (Thr^{206}–Arg^{236})		Fragment (Leu^{296}–Arg^{358})		
	M^1	P^2		M^3	P^4	M^5	P^6	M^7	P^8	
A. avenae	$[M + H]^+$	$[M + H]^+$	Δ^{1-2}	$[M + H]^+$	$[M + H]^+$	$[M + H]^+$	$[M + H]^+$	$[M + H]^+$	$[M + H]^+$	Δ^{3-4}, Δ^{5-6}, Δ^{7-8}
N1141										
Wild type	50,820	49,258	1,562	4,668	3,568	—[a]	—	6,584	6,034	1,100, —, 550
NΔFgt	49,280	49,258	22	3,567	3,568	—	—	6,034	6,034	−1, —, 0
NΔFlaA-KFlaA	51,370	49,113	2,257	4,626	3,526	3,370	2,820	6,512	5,962	1,100, 550, 550
K1										
Wild type	51,254	49,113	2,141	4,606	3,526	3,360	2,820	6,502	5,962	1,080, 540, 540
KΔFgt	49,090	49,113	−23	3,526	3,526	2,820	2,820	5,962	5,962	0, 0, 0
S178A	50,711	49,097	1,614	4,050	3,510	—	—	—	—	540, —, —
S183A	50,702	49,097	1,605	4,049	3,510	—	—	—	—	539, —, —
S212A	50,670	49,097	1,573	—	—	2,804	2,804	—	—	—, 0, —
T351A	50,649	49,083	1,566	—	—	—	—	5,930	5,932	—, —, −2
S178A/S183A/S212A/T351A	49,055	49,035	20	3,494	3,494	2,804	2,804	5,931	5,932	0, 0, −1
KΔFlaA-NFlaA	50,898	49,258	1,640	4,648	3,568	—	—	6,573	6,034	1080, —, 539

[a] —, measured molecular mass and predicted molecular mass are identical.

tin, and is expressed following N1141 flagellin infection (20). When cultured rice cells were treated with the S178A and S183A K1 flagellins and S178A/S183A K1 double substituted K1 flagellin, *Cht-1* mRNA expression was induced 6 h after treatment. In contrast, the S212A and T351A K1 flagellins did not induce remarkable *Cht-1* mRNA expression (Fig. 7*C*). These results showed that glycans at either Ser^{178} or Ser^{183} in K1 flagellin disrupt flagellin recognition in rice.

DISCUSSION

Protein glycosylation imparts novel physical properties and biological roles to both eukaryotic and prokaryotic proteins. Recently, glycoproteins from bacteria have received considerable attention, particularly glycoproteins in pathogenic species and those localized on the bacterial cell surface where they may interact with the host. In Gram-negative bacteria, examples of surface-associated glycoproteins include the pilins of *P. aeruginosa* and *Neisseria* spp. (29, 30), the adhesins TibA and Aida-1 of *E. coli* (31, 32) and HMW1 of *Haemophilus influenza* (33), and the flagellins of *A. avenae* and many other pathogenic bacteria (7, 34, 35). Although the full significance of the glycosylation of these proteins has not been determined, a number of reports have shown that these modifications are involved in virulence and motility. A glycosylation-defective mutant of *P. syringae* pv. *tabaci* retained its swimming ability but displayed defective swarming (36). The glycosylation of flagellin in several pathogens including *Campylobacter jejuni*, *Helicobacter pylori*, and *Aeromonas caviae*, which all colonize the gastrointestinal tract, is also involved in motility (37, 38). In addition, the flagellin glycans of *P. aeruginosa* and *P. syringae* pv. *tabaci* 6605 have been implicated in virulence (39, 40). We have shown that although flagellin from a K1 *Fgt* deletion mutant, *KΔFgt*, was deglycosylated the motility of the *KΔFgt* mutant was not affected. Furthermore, when rice cells were infected with the *KΔFgt* strain, this mutant produced a seedling disease characterized by the formation of brown stripes on the sheathes that was similar to the K1 wild-type strain, and both the *KΔFgt* and K1 wild-type strains had the same growth rate (supplemental Fig. 3). These data indicate that the flagellin glycan in *A. avenae* K1 strain does not influence virulence and motility. Thus, the role of the glycan in flagellin may be different in each bacterial strain, and the glycan in flagellin may play a pleiotropic role. Although the flagellin from the *KΔFgt* strain could induce the rapid immune response, such as H_2O_2 generation, the *KΔFgt* strain still caused disease in rice plant that was similar to the K1 wild-type strain. A similar observation was reported in the case of *Arabidopsis* FLS2 mutant. The pathogenic bacterium *P. syringae* pv. *tomato* DC3000 is a virulent strain to *Arabidopsis* and causes the symptom of disease. When *P. syringae* pv. *tomato* DC3000 was used to inoculate the surface of *Arabidopsis* mutated in FLS2, which is the receptor for flg22, susceptibility to this strain was increased. However, this increment of susceptibility to *P. syringae* pv. *tomato* DC3000 was only partial (41). Although the flagellin is an important pathogen-associated molecular pattern that induces several immune responses, the role of flagellin in determination of the host specificity between the plant and the pathogenic bacterial strain may be restrictive.

The bacterial flagellum is composed of a filament that is attached to a molecular motor. Flagellar filaments are composed of 11 protofilaments that wrap together to form the filament. Each protofilament is composed almost entirely of flagellin monomers that consist of four linearly connected domains, D0, D1, D2, and D3. The core D0 and D1 domains are the most highly conserved and are responsible for filament assembly. The flagellar filaments must be properly assembled for bacterial motility and polymorphisms. The middle D2 domain may affect the stability of the filament shape, and the central domains (D3) in adjacent filament subunits are not connected to each other. The D2 and D3 domains correspond with the hypervariable region located on the surface of the flagellin filament. Several lines of evidence indicate that the exposed D3 domain contains the major epitopes of the H antigen. More recent studies also suggest that Toll-like receptor 5 (TLR5), which is involved in inducing the innate immune system upon recognition of flagellin as a pathogen-associated molecular pattern, specifically recognizes the flagellin D1 domain. When the glycosylated Ser^{178} and Ser^{183} residues of the K1 flagellin of *A. avenae* were changed to alanine, both substituted flagellins induced immune

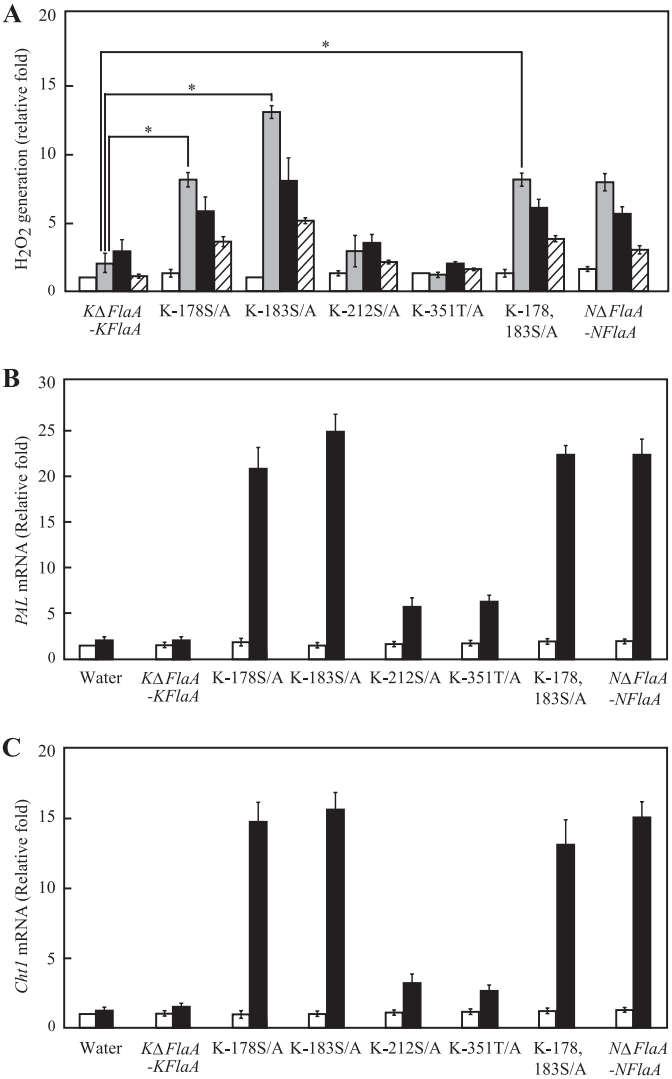

FIGURE 7. **Induction of immune responses in cultured rice cells by several mutant flagellins.** *A*, time course of H_2O_2 generation in cultured rice cells that were treated with several mutant flagellins. *White columns*, 0 h after treatment; *gray columns*, 1 h after treatment; *black columns*, 3 h after treatment; *hatched columns*, 6 h after treatment. The *y axis* represents the -fold change in H_2O_2 in cultured rice cells relative to the levels before flagellin treatment. *Asterisks* indicate a significant increase (*t* test; $p < 0.05$) in H_2O_2 generation with the amino acid-substituted flagellins. *B*, *PAL* mRNA levels in cultured rice cells that were treated with several mutant flagellins. The mRNA levels were calculated from the threshold point located in the log-linear range of RT-PCR. Standard samples with known template amounts were used to quantitate the *PAL* mRNA levels. The *y axis* represents the -fold change relative to the *PAL* mRNA levels of water-treated cultured rice cells. *White columns*, 0 h after treatment; *black columns*, 6 h after treatment. *C*, *Cht-1* mRNA levels in cultured rice cells that were treated with several mutant flagellins. The mRNA levels were calculated from the threshold point located in the log-linear range of RT-PCR. Standard samples with known template amounts were used to quantitate the *Cht-1* mRNA levels. The *y axis* represents the -fold change relative to the *Cht-1* mRNA levels of water-treated cultured rice cells. *White columns*, 0 h after treatment; *black columns*, 6 h after treatment. The *error bars* indicate the S.D. for five experiments. *KΔFlaA-KFlaA*, K1-type flagellin purified from the *KΔFlaA* strain possessing the K1 *FlaA* expression vector; *K-178S/A*, S178A substituted flagellin; *K-183S/A*, S183A substituted K1 flagellin; *K-212S/A*, S212A substituted K1 flagellin; *K-351T/A*, T351A substituted K1 flagellin; *K-178,183S/A*, S178A/S183A double substituted flagellin and N1141 flagellin purified from the *NΔFlaA* strain carrying the N1141 *FlaA* expression vector.

responses in rice. The remaining S212A and T351A K1 mutant flagellins did not induce plant immune responses. The Ser^{178} and Ser^{183} residues are located within the N-terminal D2 domain in K1 flagellin. These data indicate that the glycan moieties attached to the Ser^{178} or Ser^{183} residue in the D2 domain may be involved in flagellin recognition in rice. We demonstrated that the C-terminal D2 and D1 regions of flagellin in the *A. avenae* N1141 strain induced immune responses in cultured rice cells, whereas flagellin fragments containing the middle or N-terminal region did not induce immune responses (21). Because the D2 domain contributes to the stability of the filament shape and flagellar structure, deglycosylation of the two serine residues within the N-terminal D2 domain may cause structural changes and denudation of the epitope within the C-terminal D2 and D1 domains. Therefore, it is important to identify the detailed flagellin region recognized by rice plants and to clarify the effects of glycans on the tertiary structure of flagellin.

A structural characterization of flagellin glycosylation for a number of bacterial species has demonstrated that the glycan is linked to the protein backbone through an *O*-linkage to serine/threonine in all cases. However, a more recent study showed that the flagellin structural proteins FlaA, -B1, -B2, and -B3 and the S-layer protein of *Methanococcus voltae* are uniquely modified with a novel *N*-linked trisaccharide (34). The prokaryotic primary consensus amino acid sequence for *N*-glycosylation is (D/E)*YNX*(S/T) where *X* and *Y* can be any amino acid except proline (26). In contrast, the distinct consensus sequence for *O*-glycosylation is still unknown. The amino acid sequence of flagellin in the *A. avenae* K1 strain contains 35 asparagine residues, but there was no apparent consensus sequence for *N*-glycosylation, indicating that K1 flagellin is modified by an *O*-linked glycan. The studies have revealed significant diversity in the composition of the attached glycans. The flagellins of *C. jejuni* and *H. pylori* are glycosylated with pseudaminic acid (5,7-diacetamideo-3,5,7,9,-tetradeoxy-L-glycero-L-mannononulosonic acid) and related derivatives, whereas *Listeria monocytogenes* flagellin is glycosylated with GlcNAc, and *P. aeruginosa* type-a flagellin is glycosylated with a rhamnose-linked complex glycan (37, 42–44). More recently, flagellin of the plant pathogenic bacteria *P. syringae* pv. *tabaci* was also shown to be a glycoprotein that contains an *O*-linked trisaccharide composed of rhamnosyl and 4,6-dedeoxy-4-(3-hydroxybutanamido)-2-*O*-methylglucosyl residues (45). An analysis of the molecular mass of flagellins from K1 wild-type and *KΔFgt* mutant strains showed that Ser^{178}, Ser^{183}, Ser^{212}, and Thr^{351} are glycosylated by an ~540-Da glycan (Fig. 7). Because the molecular masses of the glycans in flagellins from *P. syringae* pv. *tabaci* and the K1 strain of *A. avenae* were accurately predicted (538 and 540 Da, respectively), the glycan moiety of K1 flagellin may be a derivative of the glycan of *P. syringae* pv. *tabaci*.

In this study, we demonstrated that the N1141-type flagellin produced by the *KΔFlaA-NFlaA* strain (N1141 *FlaA* expression vector-possessing *KΔFlaA* strain) contained a glycan of ~1,600 Da, which is the nearly same as that of the N1141 flagellin produced by the N1141 wild-type strain. Similarly, the molecular weight of the glycan attached to the K-type flagellin from the *NΔFlaA-KFlaA* strain (K1 *FlaA* expression vector-possessing *NΔFlaA* strain) is nearly the same as that of flagellin from the K1 wild-type strain (Table 2). An amino acid sequence analysis of glycosyltransferases that catalyze the transfer of the glycan

unit to serine or threonine residues in flagellin showed that the glycosyltransferases from the K1 and N1141 strains have comparatively low identity. Furthermore, *NFgt* contained an open reading frame of 4,077 bp that encoded a 1,359-amino acid protein, whereas *KFgt* is composed of 3,795 bp with 1,265 predicted amino acids. These data indicated that the glycosyltransferases of the N1141 and K1 strains catalyze the formation of the glycan linkage that is dependent on the flagellin amino acid sequence even though there are structural differences between the N1141 and K1 glycosyltransferases. Interestingly, mass spectrometry analysis using flagellins from the *NΔFlaA-KFlaA*, *KΔFlaA-NFlaA*, and wild-type strains revealed that the glycan structures in the N1141 and K1 flagellins are different because the molecular weight of the glycan in K1 flagellin was predicted to be 540, whereas the molecular weight of the glycan in N1141 flagellin was estimated to be 550. The K-type flagellin purified from the *NΔFlaA-KFlaA* strain induced immune responses, such as H_2O_2 generation, whereas the flagellin from the *KΔFlaA-KFlaA* strain did not induce H_2O_2 to the same degree as the K1 wild-type flagellin in Fig. 4*E*. These data clearly indicate that the glycan moiety linked by the K1 glycosyltransferase disrupts flagellin recognition by rice that causes the induction of immune responses. In this respect, we conclude that *O*-glycosylation of flagellin by the glycosyltransferase in the K1 strain contributes to recognition. Identifying the glycan structure associated with flagellin in the *A. avenae* K1 strain will be important to further understand how flagellin is recognized by rice.

Acknowledgments—We thank Dr. Mitsuru Yoshida for helpful discussions and Hiromi Morii for excellent technical support.

REFERENCES

1. Schwessinger, B., and Zipfel, C. (2008) *Curr. Opin. Plant Biol.* **11,** 389–395
2. Boller, T., and Felix, G. (2009) *Annu. Rev. Plant Biol.* **60,** 379–406
3. Lacombe, S., Rougon-Cardoso, A., Sherwood, E., Peeters, N., Dahlbeck, D., van Esse, H. P., Smoker, M., Rallapalli, G., Thomma, B. P., Staskawicz, B., Jones, J. D., and Zipfel, C. (2010) *Nat. Biotechnol.* **28,** 365–369
4. Jones, J. D., and Dangl, J. L. (2006) *Nature* **444,** 323–329
5. Dodds, P. N., Lawrence, G. J., Catanzariti, A. M., Teh, T., Wang, C. I., Ayliffe, M. A., Kobe, B., and Ellis, J. G. (2006) *Proc. Natl. Acad. Sci. U.S.A.* **103,** 8888–8893
6. Ade, J., DeYoung, B. J., Golstein, C., and Innes, R. W. (2007) *Proc. Natl. Acad. Sci. U.S.A.* **104,** 2531–2536
7. Logan, S. M., Hui, J. P., Vinogradov, E., Aubry, A. J., Melanson, J. E., Kelly, J. F., Nothaft, H., and Soo, E. C. (2009) *FEBS J.* **276,** 1014–1023
8. Klarzynski, O., Plesse, B., Joubert, J. M., Yvin, J. C., Kopp, M., Kloareg, B., and Fritig, B. (2000) *Plant Physiol.* **124,** 1027–1038
9. Kaku, H., Nishizawa, Y., Ishii-Minami, N., Akimoto-Tomiyama, C., Dohmae, N., Takio, K., Minami, E., and Shibuya, N. (2006) *Proc. Natl. Acad. Sci. U.S.A.* **103,** 11086–11091
10. Laquitaine, L., Gomès, E., François, J., Marchive, C., Pascal, S., Hamdi, S., Atanassova, R., Delrot, S., and Coutos-Thévenot, P. (2006) *Mol. Plant Microbe Interact.* **19,** 1103–1112
11. Silipo, A., Molinaro, A., Sturiale, L., Dow, J. M., Erbs, G., Lanzetta, R., Newman, M. A., and Parrilli, M. (2005) *J. Biol. Chem.* **280,** 33660–33668
12. Felix, G., Duran, J. D., Volko, S., and Boller, T. (1999) *Plant J.* **18,** 265–276
13. Kunze, G., Zipfel, C., Robatzek, S., Niehaus, K., Boller, T., and Felix, G. (2004) *Plant Cell* **16,** 3496–3507
14. Gómez-Gómez, L., and Boller, T. (2000) *Mol. Cell* **5,** 1003–1011
15. Chinchilla, D., Bauer, Z., Regenass, M., Boller, T., and Felix, G. (2006) *Plant Cell* **18,** 465–476
16. Kadota, I., Mizuno, A., and Nishiyama, K. (1996) *Ann. Phytopathol. Soc. Jpn.* **62,** 425–428
17. Che, F. S., Iwano, M., Tanaka, N., Takayama, S., Minami, E., Shibuya, N., Kadota, I., and Isogai, A. (1999) *Plant Cell Physiol.* **40,** 1036–1045
18. Tanaka, N., Nakajima, Y., Kaneda, T., Takayama, S., Che, F. S., and Isogai, A. (2001) *Plant Biotech.* **18,** 295–299
19. Iwano, M., Che, F. S., Goto, K., Tanaka, N., Takayama, S., and Isogai, A. (2002) *Mol. Plant Pathol.* **3,** 1–8
20. Tanaka, N., Che, F. S., Watanabe, N., Fujiwara, S., Takayama, S., and Isogai, A. (2003) *Mol. Plant Microbe Interact.* **16,** 422–428
21. Che, F. S., Nakajima, Y., Tanaka, N., Iwano, M., Yoshida, T., Takayama, S., Kadota, I., and Isogai, A. (2000) *J. Biol. Chem.* **275,** 32347–32356
22. Takai, R., Isogai, A., Takayama, S., and Che, F. S. (2008) *Mol. Plant Microbe Interact.* **21,** 1635–1642
23. Baba, A., Hasezawa, S., and Syono, K. (1986) *Plant Cell Physiol.* **27,** 463–472
24. Schwacke, R., and Hager, A. (1992) *Planta* **187,** 136–141
25. Schäfer, A., Tauch, A., Jäger, W., Kalinowski, J., Thierbach, G., and Pühler, A. (1994) *Gene* **145,** 69–73
26. Kowarik, M., Young, N. M., Numao, S., Schulz, B. L., Hug, I., Callewaert, N., Mills, D. C., Watson, D. C., Hernandez, M., Kelly, J. F., Wacker, M., and Aebi, M. (2006) *EMBO J.* **25,** 1957–1966
27. Arora, S. K., Bangera, M., Lory, S., and Ramphal, R. (2001) *Proc. Natl. Acad. Sci. U.S.A.* **98,** 9342–9347
28. Takeuchi, K., Taguchi, F., Inagaki, Y., Toyoda, K., Shiraishi, T., and Ichinose, Y. (2003) *J. Bacteriol.* **185,** 6658–6665
29. Qutyan, M., Henkel, M., Horzempa, J., Quinn, M., and Castric, P. (2010) *J. Bacteriol.* **192,** 5972–5981
30. Chamot-Rooke, J., Rousseau, B., Lanternier, F., Mikaty, G., Mairey, E., Malosse, C., Bouchoux, G., Pelicic, V., Camoin, L., Nassif, X., and Duménil, G. (2007) *Proc. Natl. Acad. Sci. U.S.A.* **104,** 14783–14788
31. Sherlock, O., Vejborg, R. M., and Klemm, P. (2005) *Infect. Immun.* **73,** 1954–1963
32. Berthiaume, F., Leblond, M. F., Harel, J., and Mourez, M. (2010) *FEMS Microbiol. Lett.* **311,** 176–184
33. Grass, S., Lichti, C. F., Townsend, R. R., Gross, J., and St Geme, J. W., 3rd (2010) *PLoS Pathog.* **6,** e1000919
34. Voisin, S., Houliston, R. S., Kelly, J., Brisson, J. R., Watson, D., Bardy, S. L., Jarrell, K. F., and Logan, S. M. (2005) *J. Biol. Chem.* **280,** 16586–16593
35. Verma, A., Schirm, M., Arora, S. K., Thibault, P., Logan, S. M., and Ramphal, R. (2006) *J. Bacteriol.* **188,** 4395–4403
36. Taguchi, F., Takeuchi, K., Katoh, E., Murata, K., Suzuki, T., Marutani, M., Kawasaki, T., Eguchi, M., Katoh, S., Kaku, H., Yasuda, C., Inagaki, Y., Toyoda, K., Shiraishi, T., and Ichinose, Y. (2006) *Cell Microbiol.* **8,** 923–938
37. Schirm, M., Soo, E. C., Aubry, A. J., Austin, J., Thibault, P., and Logan, S. M. (2003) *Mol. Microbiol.* **48,** 1579–1592
38. Ewing, C. P., Andreishcheva, E., and Guerry, P. (2009) *J. Bacteriol.* **191,** 7086–7093
39. Verma, A., Arora, S. K., Kuravi, S. K., and Ramphal, R. (2005) *Infect. Immun.* **73,** 8237–8246
40. Taguchi, F., Yamamoto, M., Ohnishi-Kameyama, M., Iwaki, M., Yoshida, M., Ishii, T., Konishi, T., and Ichinose, Y. (2010) *Microbiology* **156,** 72–80
41. Forsyth, A., Mansfield, J. W., Grabov, N., de Torres, M., Sinapidou, E., and Grant, M. R. (2010) *Mol. Plant Microbe Interact.* **23,** 1545–1552
42. Thibault, P., Logan, S. M., Kelly, J. F., Brisson, J. R., Ewing, C. P., Trust, T. J., and Guerry, P. (2001) *J. Biol. Chem.* **276,** 34862–34870
43. Schirm, M., Kalmokoff, M., Aubry, A., Thibault, P., Sandoz, M., and Logan, S. M. (2004) *J. Bacteriol.* **186,** 6721–6727
44. Schirm, M., Arora, S. K., Verma, A., Vinogradov, E., Thibault, P., Ramphal, R., and Logan, S. M. (2004) *J. Bacteriol.* **186,** 2523–2531
45. Takeuchi, K., Ono, H., Yoshida, M., Ishii, T., Katoh, E., Taguchi, F., Miki, R., Murata, K., Kaku, H., and Ichinose, Y. (2007) *J. Bacteriol.* **189,** 6945–6956